JCTC Journal of Chemical Theory and Computation

pubs.acs.org/JCTC Article

Halogen Bond of Halonium Ions: Benchmarking DFT Methods for the Description of NMR Chemical Shifts

Daniel Sethio, Gerardo Raggi, Roland Lindh,* and Máté Erdélyi*

Cite This: *J. Chem. Theory Comput.* 2020, 16, 7690−7701 Read Online

ACCESS | Metrics & More | Article Recommendations | Supporting Information

ABSTRACT: Because of their anisotropic electron distribution and electron deficiency, halonium ions are unusually strong halogen-bond donors that form strong and directional three-center, four-electron halogen bonds. These halogen bonds have received considerable attention owing to their applicability in supramolecular and synthetic chemistry and have been intensely studied using spectroscopic and crystallographic techniques over the past decade. Their computational treatment faces different challenges to those of conventional weak and neutral halogen bonds. Literature studies have used a variety of wave functions and DFT functionals for prediction of their geometries and NMR chemical shifts, however, without any systematic evaluation of the accuracy of these methods being available. In order to provide guidance for future studies, we present the assessment of the accuracy of 12 common DFT functionals along with the Hartree−Fock (HF) and the second-order Møller−Plesset perturbation theory (MP2) methods, selected from an initial set of 36 prescreened functionals, for the prediction of ^{1}H, ^{13}C, and ^{15}N NMR chemical shifts of $[N{-}X{-}N]^{+}$ halogen-bond complexes, where X = F, Cl, Br, and I. Using a benchmark set of 14 complexes, providing 170 high-quality experimental chemical shifts, we show that the choice of the DFT functional is more important than that of the basis set. The M06 functional in combination with the aug-cc-pVTZ basis set is demonstrated to provide the overall most accurate NMR chemical shifts, whereas LC-ωPBE, ωB97X-D, LC-TPSS, CAM-B3LYP, and B3LYP to show acceptable performance. Our results are expected to provide a guideline to facilitate future developments and applications of the $[N{-}X{-}N]^{+}$ halogen bond.

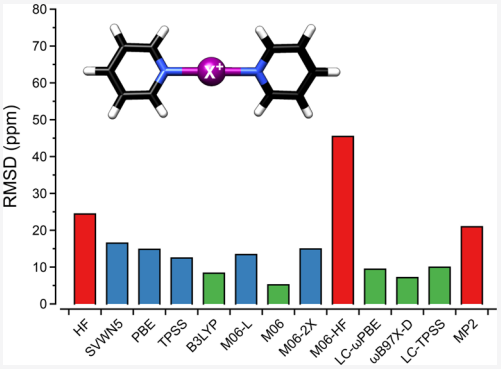

1. INTRODUCTION

Halogen bonding is the attractive interaction of the electron-depleted region of a halogen with a Lewis base.[1] As it is highly directional and resembles hydrogen bonding to a great extent, halogen bonding is applicable as a complementary tool in the modulation of molecular recognition events in chemistry and in biology. The strongest halogen-bond complexes have so far been furnished using especially electron-poor and thereby vastly electrophilic halogen-bond donors, typically obtained by perfluorination,[2] or even more efficiently using halonium ions as halogen-bond donors.[3] The halogens of the former and more extensively studied classical halogen-bond complexes possess a distinct strong covalent bond and a distinct weak halogen bond,[2] whereas those of the latter form three-center, four-electron bonds.[4] The halonium ion of such three-center bonds simultaneously interacts with two Lewis bases with comparable bond strengths and lengths.[3] Strong, three-center halogen bonds of halonium ions with nitrogen,[5−14] oxygen,[15] sulphur,[16−18] selenium,[19,20] tellurium,[21] halogen,[22] and mixed nitrogen and oxygen[23,24] electron donors have lately received ample attention and also found applications in supramolecular chemistry, for example.[3,18,25−29] Although the halogen bond of neutral organic halogen bond donors, such as of iodoperfluorocarbons, is weak (<10 kJ/mol),[30] those of halonium ions are typically >50 kJ/mol and often even >100 kJ/mol.[3,31] This strength is expected to originate from the vast electron deficiency of halonium ions, as compared to the slight electrophilicity of common neutral halogen-bond donors.[2] Their positive charge makes halonium ions to exceptionally strong halogen-bond donors. Accordingly, the halogen bonds of halonium ions have been reported to possess remarkably short donor−acceptor distances (R_{XB} = 0.65−0.69, where $R_{XB} = d_{XB}/(X_{vdW} + B_{vdW})$),[3] as compared to conventional neutral halogen bonds (R_{XB} > 0.9). The halogen bonds involving a charged species are expected to possess a larger electrostatic character and thereby act over longer distances. Thereto, induction is expected to play a more prominent role for charged as compared to neutral species.[32] Overall, the strong, three-center halogen bond of halonium ions shows a number of features different from those of conventional, weak halogen

Received: August 19, 2020
Published: November 2, 2020

https://dx.doi.org/10.1021/acs.jctc.0c00860
J. Chem. Theory Comput. 2020, 16, 7690−7701

bonds. Its description may therefore need different computational treatment, for instance, for the accurate estimation of the chemical shift of atoms involved or nearby the interaction.

Conventional halogen bonds, D−X···D (where D acts as an electron donor, whereas X is a halogen that acts as an electron acceptor), have been extensively studied, computations greatly supporting the interpretation of experimental observations[2,33] and the overall understanding of the halogen-bonding phenomenon.[34] For such conventional bonds, extensive benchmarking studies have been carried out, surveying the accuracy of a wide set of DFT methods and wave functions[35,36] and providing guidance for further investigations. The strong, three-center halogen bond of halonium ions has been repeatedly reviewed from an experimental perspective;[3,37,38] however, in contrast, its computational treatment has so far received less attention. Apart from scarce examples of entirely theoretical studies,[39,40] most investigations analyzing three-center halogen bonds used DFT predominantly to support the interpretation of experimental data, most often of NMR chemical shifts obtained in solutions.[3,5−11,15,41] In the past decade, diverse computational methods (DFT functionals and basis sets) have been used, however, without giving any guidance on or evaluation of the applied methods' accuracy regarding the computed spectroscopic parameters or the geometry and the energy of such complexes.[5−15,39−42] The DFT description of three-center, four-electron halogen bonds is challenging because of the self-interaction error inherent to DFT[43] and to the incomplete description of nondynamic electron correlations in these bonds.[44] Unsurprisingly, discrepancies between experimental observations and computational results have been reported in some cases.[12]

In earlier work, we assessed B3LYP against B3LYP-D3, MP2, and M06-2X[8] and compared the outcome to independent CCSD(T) calculations.[42] We have shown that the contribution of dispersion to the overall interaction energy of three-center halogen bonds, $[D-X-D]^+$, is minor, in contrast to its major impact for conventional neutral and weak halogen bonds, D−X···D.[8] This is due to the partial ionic character, unusual strength, and shortness of the halogen bonds of halonium ions.[3] Moreover, we proved the influence of basis-set superposition error (BSSE) to be negligible.[5] Herein, we report the comprehensive assessment of the accuracy of DFT methods and two wave functions (HF and MP2) for the description of NMR chemical shifts of three-center, four-electron halogen-bond systems, that is, the exceptionally strong halogen-bond complexes of halonium ions. For this investigation, we used the three-center, four-electron halogen-bond model systems that have so far been experimentally most extensively studied (Figure 1)[3,10,37] and have also been used as benchmark systems in various contexts,[4,45,46] providing ample and reliable experimental data for comparison. As the counterion has previously been demonstrated to not influence $[N-I-N]^+$ halogen bonds significantly, it was omitted in the current calculations.[9]

2. COMPUTATIONAL DETAILS

The geometries of $[N-X-N]^+$ complexes were optimized at the ωB97X-D/aug-cc-pVTZ level of theory. The ωB97X-D functional was chosen as it is known to adequately account for electron correlations for systems exhibiting noncovalent interactions[47,48] including halogen bonding.[35,49] Dichloromethane solvation effects were included using the polarizable continuum model (PCM) of Tomasi and co-workers.[50] For

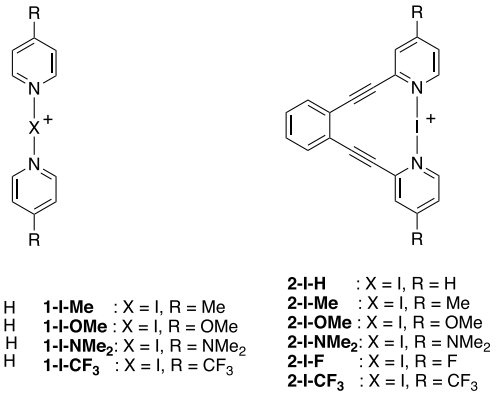

Figure 1. Schematic representation of the three-center, four-electron $[N-X-N]^+$ halogen-bond complexes studied in the present work.

geometry optimization, the substrate solvation cavities were modeled using the united-atomic radii (UA0), while for chemical shielding calculations, the substrate solvation cavities were modeled using the Bondi atomic radii[51] as suggested by Willoughby and co-workers.[52] Vibrational frequency calculations were followed at the same level of theory to ensure the optimized geometry corresponding to geometry minima.

Chemical shielding constants (σ) were obtained at the GIAO-HF, GIAO-MP2, and GIAO-DFT levels.[53−55] For the two former, two wave function methods were used including HF[56] and MP2.[57] For the latter, 12 commonly used functionals were used including an LSDA (SVWN5[58,59]), a GGA (PBE[60,61]), a meta GGA (TPSS[62]), a hybrid (B3LYP),[63,64] four long-range-corrected functionals (CAM-B3LYP,[65] LC-ωPBE,[66−68] ωB97X-D,[69] and LC-TPSS[70]) as well as four Truhlar's functionals of the M06 family: M06-L,[71] M06,[72] M06-2X,[72] and M06-HF.[73]

Three different basis sets of triple-ζ-polarized quality augmented with diffuse functions were employed for describing the C, H, O, N, F, Cl, Br, and I atoms: the Pople's 6-311++G(d,p),[74,75] the Ahlrichs' def2-TZVP,[76,77] and the Dunning's aug-cc-pVTZ[78,79] basis sets. For heavy atoms (e.g., I), scalar relativistic effects were assessed by two effective core potentials (ECPs): (i) the Stuttgart−Dresden (SDD)[80,81] and (ii) the Los Alamos National Laboratory (LANL2),[82] where the former is superior compared with the latter. The small-core relativistic pseudopotentials of SDD have been carefully designed to explicitly treat the Pauli repulsion of the cores, their Coulombic and exchange effects on the valence space, and the scalar relativistic corrections as well as their two-component extensions describing outer-core and valence spin−orbit interactions.[81] As we calculated the NMR shielding tensors at the chemical equilibrium geometries, we expect that the use of small-core relativistic pseudopotentials handle the heavy-atom light-atom (HALA) effects to some extent. The remaining HALA effects, which cannot be handled by relativistic ECP, may explain the discrepancy between the calculated and the experimental values to some extent. Although the ^{1}H and ^{13}C NMR chemical shifts are dominated by the diamagnetic term in the shielding constants, ^{15}N NMR chemical shifts have been previously shown to be determined by the paramagnetic term. This has earlier been discussed by Pazderski,[83] for example.

To evaluate the performance of different methods and basis sets, we used the root mean square deviation (rmsd) and the

https://dx.doi.org/10.1021/acs.jctc.0c00860
J. Chem. Theory Comput. 2020, 16, 7690−7701

normalized root mean square deviation (|rmsd|), which were computed as follows over N nuclei

$$\mathrm{rmsd} = \sqrt{\frac{\sum_N (\delta_{\mathrm{calc.}} - \delta_{\mathrm{exp.}})^2}{N}} \quad (1)$$

$$|\mathrm{rmsd}| = \left(\frac{\mathrm{rmsd}}{\sum \mathrm{rmsd}}\right)_{^1\mathrm{H}} + \left(\frac{\mathrm{rmsd}}{\sum \mathrm{rmsd}}\right)_{^{13}\mathrm{C}} + \left(\frac{\mathrm{rmsd}}{\sum \mathrm{rmsd}}\right)_{^{15}\mathrm{N}} \quad (2)$$

where $\delta_{\mathrm{calc.}}$ and $\delta_{\mathrm{exp.}}$ are the calculated and experimental chemical shifts, respectively.

All calculations were performed using the Gaussian 16 Rev. C.01 package.[84] The geometry optimization and NMR chemical shift calculations were performed using ultrafine grid integration and tight convergence criteria for the forces and displacement.[85] For the NBO analysis[86,87] of [bis(pyridine)iodine(I)]-type complexes, we direct the reader to refs 8, 10.

3. RESULTS AND DISCUSSION

We assessed the performance of 12 commonly used DFT functionals as well as of two wave function methods with regard to their capability of reproducing experimental ^{1}H, ^{13}C, and ^{15}N NMR chemical shifts of three-center, four-electron [N−X−N]$^+$ halogen-bond complexes. We also evaluated the performance of three different families of basis sets utilizing six selected functionals.

3.1. Test Set. For the evaluation of computational methods' ability to accurately describe the NMR chemical shifts of three-center, four-electron [N−I−N]$^+$ halogen-bond complexes, a set of 14 systems (Figure 1) providing 170 reliable experimental NMR chemical shift values[8,10] was selected. The calculated ^{1}H, ^{13}C, and ^{15}N chemical shielding tensors (σ) were converted into ^{1}H, ^{13}C, and ^{15}N chemical shifts (δ in ppm, where $\delta = \sigma_{\mathrm{ref}} - \sigma$) utilizing the proton and carbon atoms of tetramethylsilane (TMS) as a reference for ^{1}H and ^{13}C NMR chemical shifts and the nitrogen of nitromethane as a reference for ^{15}N NMR chemical shifts. As the experimental chemical shifts were obtained in dichloromethane-d_2 solution, the corresponding implicit solvent model was used. Calculated and experimental ^{1}H, ^{13}C, and ^{15}N NMR chemical shifts are given for all discussed halogen-bond complexes in the Supporting Information.

3.2. Exchange−Correlation Functionals. DFT is widely known as an inexpensive method for calculating NMR chemical shifts. As previously shown by Stoychev and co-workers, the choice of the method is the main source of error and the accuracy varies depending mainly on the choice of functionals.[88] Following a prescreening of 36 functionals utilizing **1-I−H**[89] as well as two wave function (HF and MP2) methods, we selected 12 commonly used functionals for further evaluation. To avoid any bias arising from molecular conformational changes, that is, molecular vibrations,[90] the shielding constants were calculated with equilibrium geometries obtained at the ωB97X-D/aug-cc-pVTZ level of theory. This geometry is in excellent agreement with the experimentally obtained X-ray structure,[91] as indicated by the rmsd of 0.1036 for complex **1-I−H** (Figure 2). The rmsd of ^{1}H, ^{13}C, and ^{15}N NMR chemical shifts with respect to the experimental values is shown in Figure 3. Explicit NMR chemical shifts for all considered nuclei on all levels of theory discussed here are given in the Supporting Information.

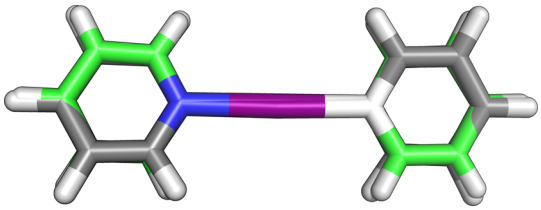

Figure 2. Superimposed geometries of complex **1-I−H** determined by single-crystal X-ray diffraction (gray) and DFT (green).

All methods perform reasonably well in reproducing experimental ^{1}H chemical shifts as indicated by the rmsd values ranging from 0.25 to 1.47 ppm (Figure 3a), with the M06-HF functional providing the least accurate prediction, yielding an rmsd of 1.47 ppm. It is worth noting that HF shows comparable accuracy to DFT and MP2, which is in agreement with the previous work of Flaig and co-workers.[92] The best match to the experimental ^{1}H NMR chemical shifts is obtained when using the TPSS, M06-L, PBE, or B3LYP functionals.

For ^{13}C NMR chemical shifts, a larger variance in accuracy is observed, as reflected by the rmsd values ranging from 2.74 to 51.48 ppm (Figure 3b). The good performance of PBE and TPSS functionals has been pointed out by previous studies[88,93] and is in agreement with our observation of the PBE, TPSS, and M06 functionals achieving the lowest rmsd values. The inclusion of HF exchange improves the calculated NMR shifts for the M06 family (M06-L: 0% HF exchange, M06: 27% HF exchange, M06-2X: 54% HF exchange, and M06-HF: 100% HF exchange), with the optimum of 27% HF exchange obtained with the M06 functional.[94−97] However, the inclusion of 100% of HF exchange in M06-HF lowers the quality of the chemical shift prediction. This observation agrees with the recent finding by Truhlar and co-workers that an excessive inclusion of HF exchange amplifies the static correlation error.[98] This is due to the HF exchange deteriorating the ability of local exchange in DFT functionals to account for the localization effects associated with static correlation. MP2 shows good performance, with an rmsd of 4.56 ppm over the entire set of studied complexes.[99−101]

An even larger quality variation of prediction is observed for ^{15}N NMR chemical shifts, in line with previous reports.[102−104] The rmsd values range from 7.04 to 79.48 ppm, with the M06 and LC-TPSS functionals performing the best (rmsd of M06 7.94 and of LC-TPSS 7.04 ppm), comparable to that of the previously suggested KT3/pcS-3 method.[105] HF and MP2 are among the methods least reliably describing the ^{15}N NMR chemical shifts of these systems. Similar to that observed for ^{13}C NMR chemical shift predictions mentioned above, the inclusion of HF exchange leads to an improvement of the calculated ^{15}N NMR chemical shifts, with the optimum being seen for 27% HF exchange included in the M06 functional.

The quality of prediction of ^{15}N NMR chemical shifts is strikingly lower than those of ^{1}H and ^{13}C NMR shifts (Figure 3) that is explained by the widely acknowledged shortcoming of DFT at describing charge-transfer interactions.[106] Thus, the energy of charge-transfer states is typically strongly underestimated because of the incomplete compensation of electron self-repulsion by the approximate exchange−correlation functional, while HF typically strongly overestimates it. As the nitrogen atoms are directly involved in the charge-transfer

https://dx.doi.org/10.1021/acs.jctc.0c00860
J. Chem. Theory Comput. 2020, 16, 7690−7701

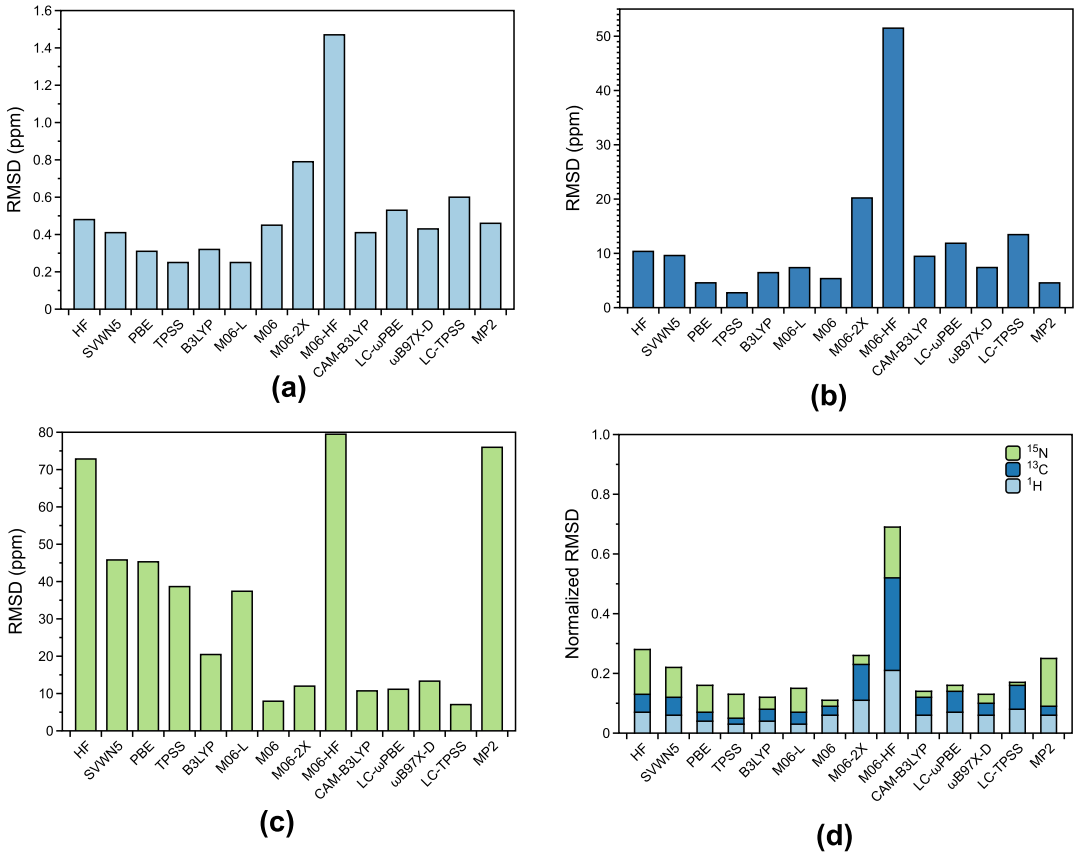

Figure 3. Rmsd of the predicted NMR chemical shifts with respect to experimental values for 14 $[N-I-N]^+$ halogen-bond complexes (Figure 1), evaluating the performance of 12 DFT functionals as well as of HF and MP2. (a) ^{1}H NMR chemical shifts. (b) ^{13}C NMR chemical shifts. (c) ^{15}N NMR chemical shifts. (d) ^{1}H, ^{13}C, and ^{15}N NMR chemical shifts.

interaction, here termed halogen bonding, their chemical shift calculations are affected the most. A substantial electron transfer in the charge-transfer complexes of pyridines has previously been demonstrated.[107,108] Moreover, the discrepancy of the predicted ^{15}N NMR chemical shifts can also be attributed to (i) the remaining HALA effects which cannot be handled by relativistic ECP, (ii) zero-point vibrations for temperature corrections, and (iii) the incomplete description of nondynamical electron correlations in these bonds. The good performance of the M06 functional is thus not unexpected, as this method has been specifically designed to deal with the self-interaction error, thereby compensating this weakness.[109] The observation of improved accuracy of ^{15}N NMR chemical shift prediction upon adjustment of HF exchange further corroborates this explanation.

The maximum deviations in the prediction of the chemical shifts of all three nuclei, given in Table 1, support the abovementioned conclusions. Hence, M06-HF provides by far the poorest performance for ^{1}H NMR chemical shifts, whereas TPSS, M06-L, PBE, and B3LYP give the most accurate predictions. For ^{13}C NMR chemical shifts, TPSS, PBE, M06, MP2, and B3LYP are the most accurate, whereas M06-HF remains giving the largest deviations from reality. In our hands, the most accurate ^{15}N NMR chemical shifts were predicted by LC-TPSSS, M06, M06-2X, CAM-B3LYP, and LC-ωPBE, whereas a large number of functions appear to not be applicable for the prediction of ^{15}N NMR data for halonium ions' halogen-bond complexes.

Table 1. Maximum Absolute Deviations from the Experimental Values of 14 $[N-I-N]^+$ Halogen-Bond Complexes of the Predicted ^{1}H, ^{13}C, and ^{15}N NMR Chemical Shifts for 12 DFT Functionals as Well as HF and MP2 (in ppm)

functional	^{1}H	^{13}C	^{15}N
HF	0.66	15.96	73.90
SVWN	0.58	13.48	50.70
PBE	0.46	7.79	50.25
TPSS	0.38	5.36	42.98
B3LYP	0.46	8.59	21.77
M06-L	0.38	12.19	41.34
M06	0.57	8.27	6.44
M06-2X	0.98	24.65	9.95
M06-HF	1.85	67.01	80.83
CAM-B3LYP	0.56	12.33	9.70
LC-ωPBE	0.71	15.65	10.40
ωB97X-D	0.59	10.07	13.10
LC-TPSSS	0.78	17.79	4.98
MP2	0.69	8.37	81.65

Overall for ^{1}H, ^{13}C, and ^{15}N NMR chemical shifts, the M06 functional performs best among the 12 functionals studied here, offering a reasonable balance between cost and accuracy. Although it does not offer the lowest error in prediction of ^{1}H chemical shifts, the outcome is acceptable and simultaneously it is clearly among the best for prediction of ^{13}C and by far the very best for ^{15}N NMR chemical shift prediction. B3LYP and the four long-range-corrected functionals CAM-B3LYP, LC-

https://dx.doi.org/10.1021/acs.jctc.0c00860
J. Chem. Theory Comput. 2020, 16, 7690−7701

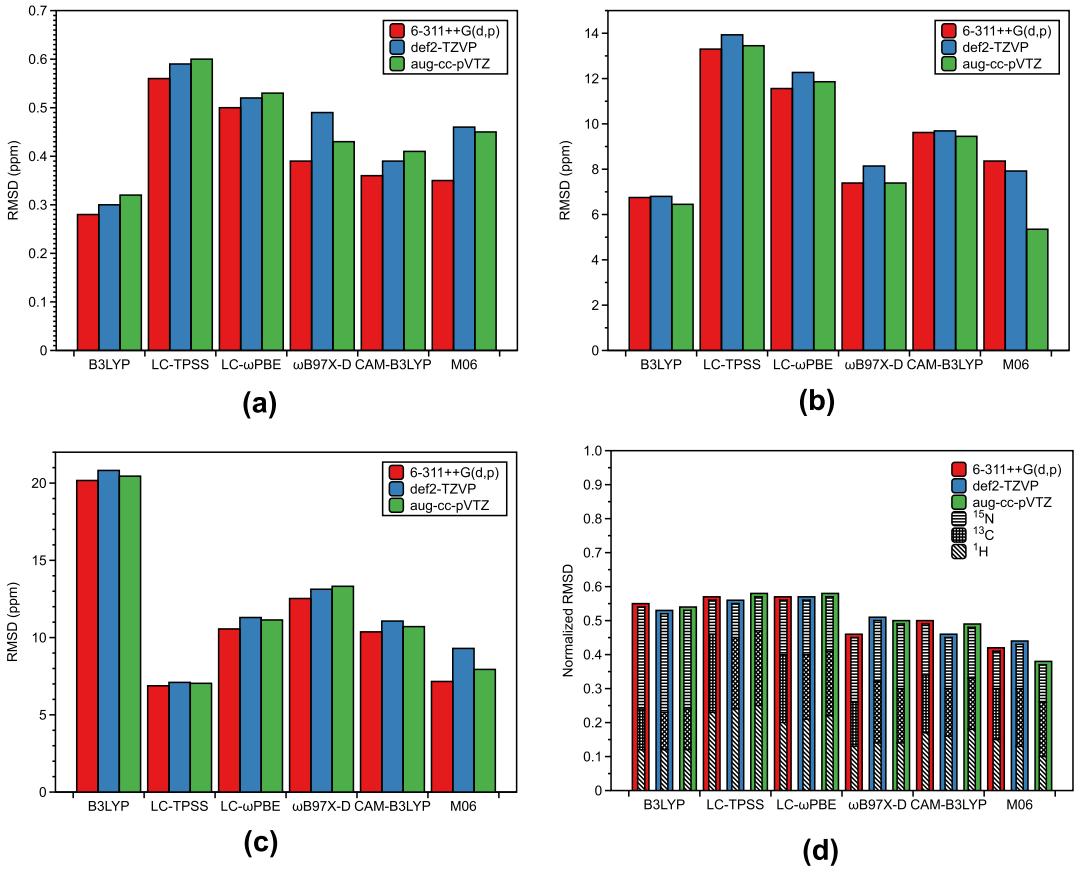

Figure 4. Rmsd of the predicted NMR chemical shifts with respect to experimental values for 14 $[N-I-N]^+$ halogen-bond complexes (Figure 1), evaluating three different basis sets. (a) ^{1}H NMR chemical shifts. (b) ^{13}C NMR chemical shifts. (c) ^{15}N NMR chemical shifts. (d) ^{1}H, ^{13}C, and ^{15}N NMR chemical shifts.

ωPBE, ωB97X-D, and LC-TPSS perform reasonably well and hence may be used without taking larger risks.

3.3. Basis Sets. Pople's 6-311++G(d,p), Ahlrichs' def2-TZVP, and Dunning's aug-cc-pVTZ, three of the most commonly used basis sets of triple-ζ-polarized quality augmented with diffuse functions, were evaluated for their performance using the six best performing functionals B3LYP, CAM-B3LYP, LC-TPSS, LC-ωPBE, ωB97X-D, and M06. We chose triple-ζ-quality basis sets as these are known to provide a good compromise between accuracy and cost,[110] whereas those beyond triple-ζ do not significantly improve the accuracy.[110,111] Those of lower quality were expected to not yield reliable enough predictions and were therefore omitted.[110]

In our hands, all three basis sets showed comparable performance in describing ^{1}H and ^{15}N NMR chemical shifts (Figure 4) with 6-311++G(d,p) typically providing slightly better results than def2-TZVP and aug-cc-pVTZ. However, at the prediction of ^{13}C NMR chemical shifts, the Dunning's aug-cc-pVTZ performs somewhat better as compared to 6-311++G(d,p) and def2-TZVP, whose observation is in line with a previous report by Iron.[110] The Dunning's basis set is superior for this purpose, even over Jensen's pcS-n[112] and pcSseg-n[113] basis sets that have been designed specifically for prediction of NMR chemical shifts.[110] The comparison of the predicted chemical shifts obtained with Dunning's aug-cc-pVTZ basis set with those obtained using mixed basis sets of Pople's 6-311+G(d,p) for I and Jensen's aug-pc-2 for H and N demonstrates the Dunning's basis set to be superior (Supporting Information Table S30).[11] Further tests on complex **1-F−H** and **1-Cl−H** utilizing aug-pcSseg-3 indicated severe self-consistent field (SCF) convergence problems, whereas the influence of improved core−valence (aug-cc-CVTZ) was found to be negligible.[110]

Altogether, when predicting both ^{1}H, ^{13}C, and ^{15}N NMR chemical shifts, the Dunning's aug-cc-pVTZ, which possesses high-quality polarization and diffuse functions, performs the best among the three families of basis sets studied here. This is clearly the first choice for ^{13}C NMR prediction, whereas 6-311++G(d,p) is for ^{1}H NMR. For the prediction of ^{15}N NMR chemical shifts, the choice of the basis set appears to not play a significant role.

3.4. Halogen. The relative contribution of charge transfer to the three-center, four-electron halogen-bond interaction has been shown to depend on the type of halogen involved.[3,8] We, therefore, compared the quality of chemical shift prediction as a function of the identity of the central halogen(I) for the abovementioned 12 DFT functionals as well as for HF and MP2 (Figure 5). For ^{1}H NMR chemical shifts, the highest quality of prediction was observed for the chlorine(I)-centered complexes, independent of the functional, followed by bromine(I) and iodine(I), for which the variance in accuracy is comparable. The lowest accuracy is seen for prediction of fluorine-centered halogen bonds, which in turn are vastly different in character from the halogen bonds of the other three halogens.[4,8] The accuracy of ^{13}C NMR chemical shift prediction for $[N-X-N]^+$ halogen bonds appears virtually independent of the type of halogen involved (Figure 5b). Apart

https://dx.doi.org/10.1021/acs.jctc.0c00860
J. Chem. Theory Comput. 2020, 16, 7690−7701

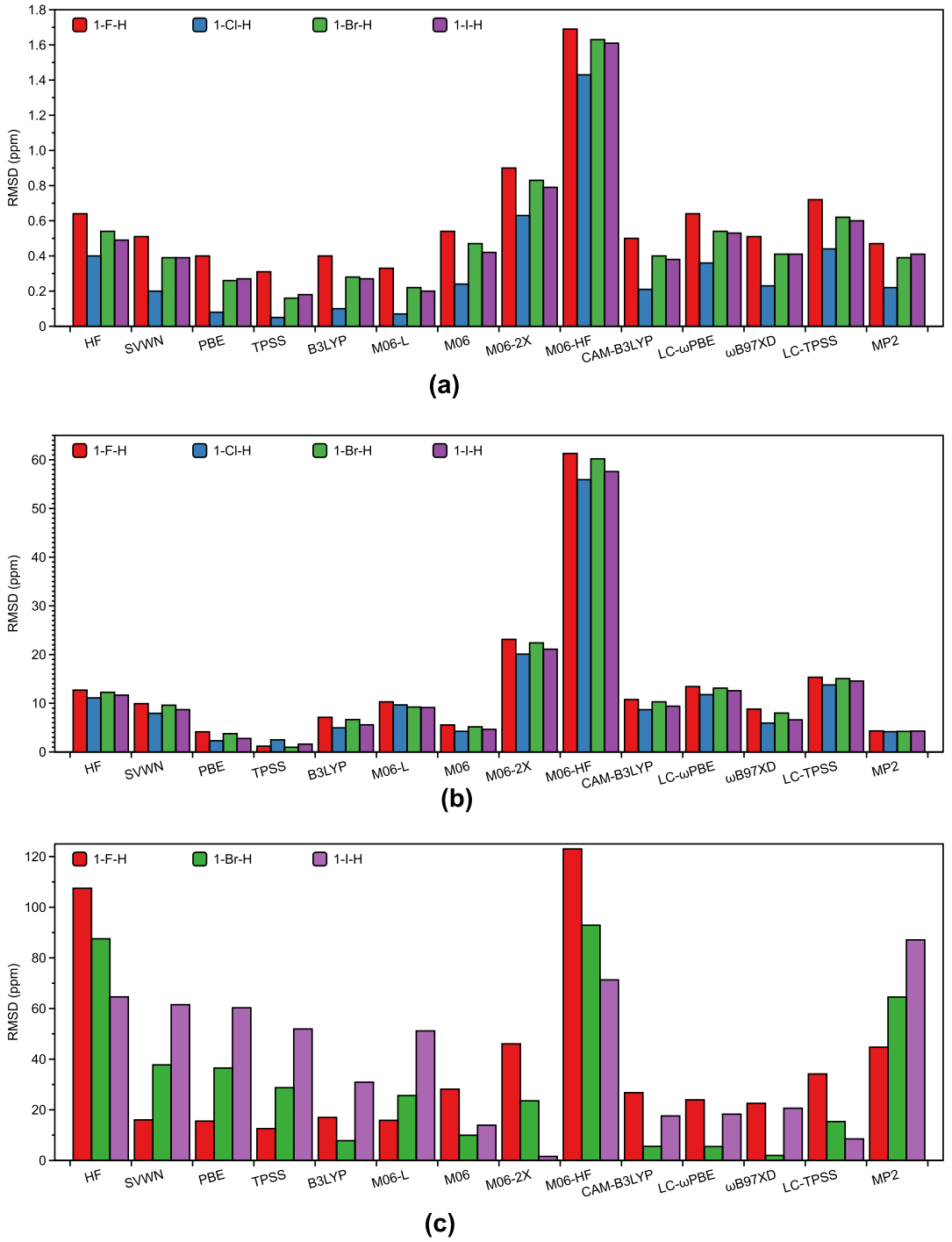

Figure 5. Rmsd of the predicted NMR chemical shifts with respect to experimental values for 4 $[N-I-N]^+$ halogen-bond complexes (Figure 1), evaluating the performance of 12 DFT functionals as well as HF and MP2. The rmsd of ^{15}N NMR chemical shifts of Cl-centered complexes are omitted because of the unavailability of a larger set of experimental data.[3,8] (a) ^{1}H NMR chemical shifts. (b) ^{13}C NMR chemical shifts. (c) ^{15}N NMR chemical shifts.

from the strikingly low-quality predictions by HF and M06-HF, the error of ^{15}N NMR chemical shift prediction is typically the largest for the iodine(I)-centered bonds; however, the trends are less uniform, with LC-TPSS showing the opposite order of accuracy for the different halogens than M06-L, for example. Altogether, the optimal choice of the functional is here demonstrated to be more halogen-dependent for the ^{15}N NMR chemical shift prediction than for the ^{1}H NMR and especially for the ^{13}C NMR chemical shift predictions.

3.5. Electron Density. The electron density of the halogen-bond acceptor Lewis base is known to influence halogen-bond strength,[2,10] and therefore, we evaluated whether the electron density of the studied systems may modulate the accuracy of the chemical shift prediction. Whereas the prediction of ^{1}H and ^{13}C NMR chemical shifts showed little dependence on the electron density of the pyridines (typically <0.2 ppm variation of error for ^{1}H NMR and <2 ppm for ^{13}C NMR, Figure 6), that of the ^{15}N NMR chemical shift showed

https://dx.doi.org/10.1021/acs.jctc.0c00860
J. Chem. Theory Comput. 2020, 16, 7690−7701

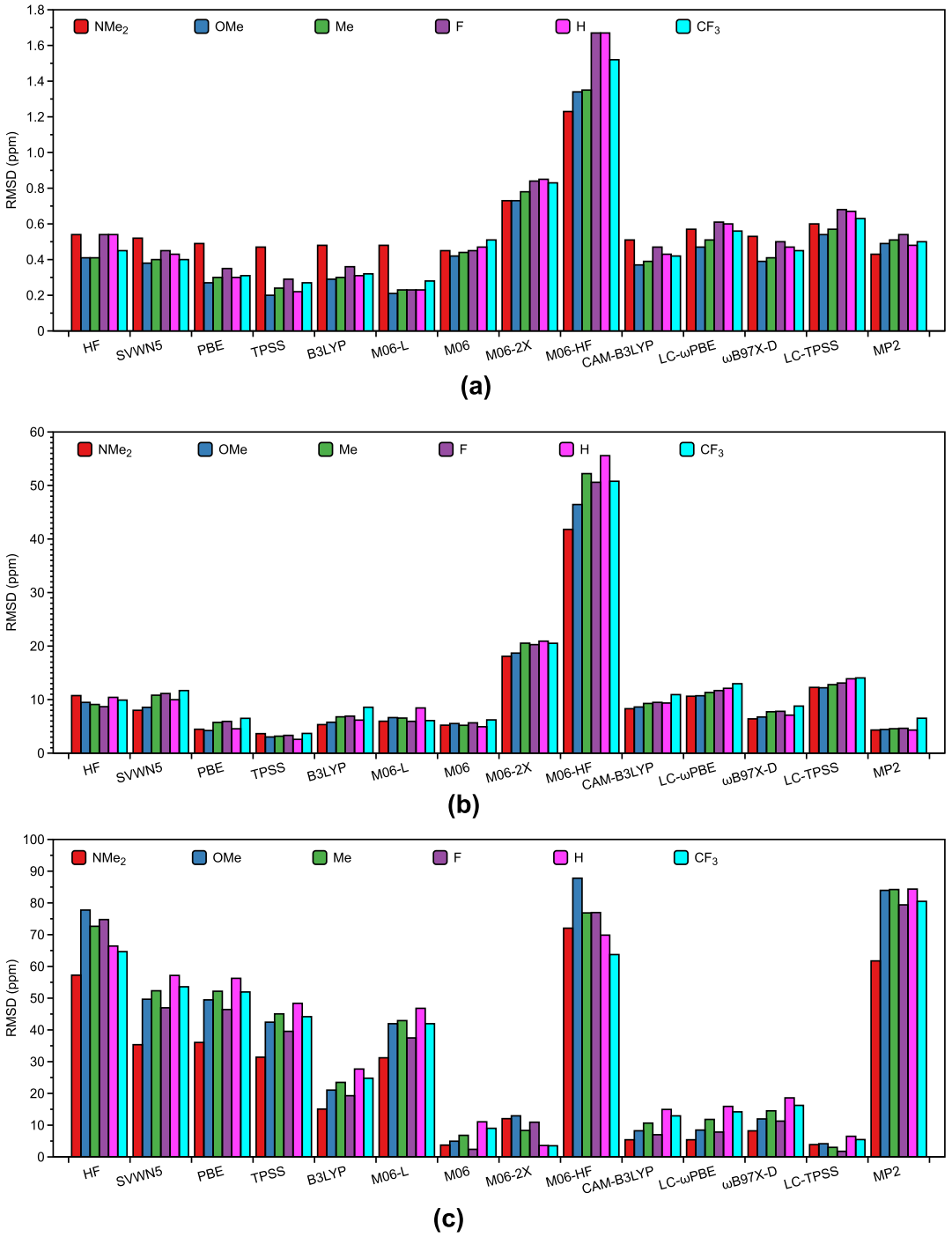

Figure 6. Rmsd of the predicted NMR chemical shifts with respect to experimental values for 6 $[N{-}I{-}N]^+$ halogen-bond complexes (Figure 1), evaluating the performance of 12 DFT functionals as well as HF and MP2. (a) ^{1}H NMR chemical shifts. (b) ^{13}C NMR chemical shifts. (c) ^{15}N NMR chemical shifts.

>5 ppm variation. Different functionals exhibit somewhat dissimilar behavior; however, overall, the accuracy of ^{15}N NMR chemical shift prediction appears to be to some extent better for the most electron-rich NMe_2-substituted $[N{-}I{-}N]^+$ complex, which possesses the strongest halogen bond, for most of the studied functions. All in all, the choice of the DFT functional has a larger influence on the quality of the outcome than the electron density of the halogen-bond complex. In our hands, the choice of the basis set does not have a significant impact on the quality of NMR chemical shift predictions, neither upon variation of nuclei (Figures S29 and S45) nor upon altering the electron density (Figures S30 and S46).

An NBO analysis of the 1-I−R complexes (Figure 1) corroborates our earlier findings that the halogen bonds of halonium ions have a strong charge-transfer character.[8] The iodine(I) of the $[N{-}X{-}N]^+$ complexes transfers 0.55−0.59 positive charge to the pyridine rings (Table 2). Our data suggest that the delocalization from the N lone-pair orbitals into the N−X ps* bond orbital is the dominant contribution to the stabilization of the three-center, four-electron halogen bond. The extent of charge transfer depends on the electronic

https://dx.doi.org/10.1021/acs.jctc.0c00860
J. Chem. Theory Comput. 2020, 16, 7690−7701

Table 2. Bond Distances (in Å), Natural Charge Analysis (in e), and Second-Order Perturbation of the Fock Matrix between the Nitrogen Lone Pair and the Accepting Central Atom (in kcal/mol) Calculated at the ωB97X-D/aug-cc-pVTZ-pp Level of Theory

complex	R_{N-I} (Å)	q_N	q_I	$n_N \rightarrow n_{(s,p)}$
1-I−NMe_2	2.259	−0.536	+0.411	
1-I−OMe	2.264	−0.506	+0.423	151.00
1-I−Me	2.267	−0.482	+0.426	149.53
1-I−H	2.269	−0.476	+0.434	146.94
1-I−CF_3	2.272	−0.459	+0.446	144.04

character of the para-substituent of the 1-I−R complexes and hence on the electron density of the Lewis basic nitrogen.[10,11] Most extensive charge transfer is observed for the most electron-rich 1-I−NMe_2, whereas the least for the most electron-poor 1-I−CF_3 complex. An increase in charge-transfer character of 1-I−R complexes is seen to be associated with the shortening of the N−I bond (R_{N-I}) and hence with an increase in bond strength. This is in agreement with previous experimental observations.[10,11] Simultaneously, the Coulombic character of the bond decreases. It is worth noting that a gradual increase in charge delocalization (I 0.59, Br 0.72, and Cl 0.84) and simultaneous decrease in electrostatic character of the halogen bond have previously been reported upon the decrease in halogen size,[3,8] which was associated with the weakening of the interaction (I > Br > Cl).

4. SUMMARY

Evaluation of the capability of functionals and basis sets to predict NMR chemical shifts of three-center, four-electron halogen-bond complexes revealed the M06 exchange−correlation functional to give the overall best performance. Most functionals except M06-HF and M06-2X reproduce ^{1}H and ^{13}C NMR chemical shifts for this type of halogen-bond complexes reasonably well. It is worth noting that HF and MP2 provide comparably accurate predictions to DFT for ^{1}H and ^{13}C but not for ^{15}N NMR chemical shifts. We found that only six of the DFT functionals (M06, B3LYP, CAM-B3LYP, LC-ωPBE, ωB97X-D, and LC-TPSS) gave reasonably good accuracy at the prediction of ^{15}N NMR chemical shifts for $[N-I-N]^+$ halogen-bond complexes. B3LYP's prediction accuracy is overall poorer, even if it by far outperforms a number of other functionals. In addition, the four long-range-corrected functionals LC-ωPBE, ωB97X-D, LC-TPSS, and CAM-B3LYP as well as B3LYP (^{1}H and ^{13}C) show acceptable performance for strong three-center halogen-bond complexes. According to the commonly accepted "Jacob's ladder" specification of functionals, accurate prediction of NMR chemical shifts for $[N-I-N]^+$ complexes is achieved when functionals of rung-4 and above are applied.[114] Even if a certain functional may provide the best result for a certain nucleus, altogether, we recommend the use of the M06 method because of its ability to provide reliable chemical shift predictions for ^{1}H, ^{13}C, and ^{15}N NMR with consistent accuracy. As the ^{1}H and ^{13}C NMR chemical shifts are much better reproduced by most methods than the ^{15}N NMR shifts, the computation of the latter data directs the selection of the functional.

The choice of the basis set has a lower influence on the quality of the prediction than that of the functional. According to our findings, the combination of the M06 functional with the aug-cc-pVTZ basis set provided the overall most accurate data for ^{1}H, ^{13}C, and ^{15}N NMR chemical shift prediction. The prediction of ^{15}N NMR chemical shifts is much less accurate than those of ^{1}H and ^{13}C NMR chemical shifts. The type of halogen and the electron density of the complex do not have a significant influence on the accuracy of the predictions. In contrast to conventional halogen bonds,[35] the use of M06-L and M06-2X functionals is not advisable, whereas ωB97X-D appears to provide a reasonably good prediction for both conventional, weak, and for strong three-center halogen-bond complexes. It should be kept in mind that in contrast to the computation of conventional halogen bonds,[35] dispersion and basis set superposition error are of insignificant importance[8] at the description of the strong, charged three-center, four-electron halogen bonds of halonium ions. Double hybrid functionals were recently shown to provide promising accuracy at chemical shift prediction when compared to CCSD(T) benchmark data,[115] however, are not yet implemented in the Gaussian 16 Rev. C.01 package for calculations of NMR shielding tensors, which was used in this investigation.

We expect that the practical guideline provided here will serve as a useful tool for the continued structural investigations and applications of three-center, four-electron $[N-X-N]^+$ halogen-bond complexes. This motif has recently evolved into a useful supramolecular synthon, a mild synthetic agent for halonium transfer reactions, and an instructive model system for gaining further understanding of the chemical bonding phenomenon.[3,4]

■ ASSOCIATED CONTENT

Supporting Information

The Supporting Information is available free of charge at https://pubs.acs.org/doi/10.1021/acs.jctc.0c00860.

Performance of 11 DFT functionals, HF, and MP2; performance of the 6-311++G(d,p) basis set; performance of the def2-TZVP basis set; and optimized geometries obtained at the ωB97X-D/aug-cc-pVTZ level of theory (PDF)

■ AUTHOR INFORMATION

Corresponding Authors

Roland Lindh − *Department of Chemistry—BMC, Uppsala University, 751 23 Uppsala, Sweden;* orcid.org/0000-0001-7567-8295; Email: roland.lindh@kemi.uu.se

Máté Erdélyi − *Department of Chemistry—BMC, Uppsala University, 751 23 Uppsala, Sweden;* orcid.org/0000-0003-0359-5970; Email: mate.erdelyi@kemi.uu.se

Authors

Daniel Sethio − *Department of Chemistry—BMC, Uppsala University, 751 23 Uppsala, Sweden;* orcid.org/0000-0002-8075-1482

Gerardo Raggi − *Department of Chemistry—BMC, Uppsala University, 751 23 Uppsala, Sweden*

Complete contact information is available at: https://pubs.acs.org/10.1021/acs.jctc.0c00860

Notes

The authors declare no competing financial interest.

■ ACKNOWLEDGMENTS

The authors thank Marcus Reitti, Jürgen Gräfenstein, Ulrika Brath, and Stefano Battaglia for fruitful discussion. D.S. thanks

Vasanthanathan Poongavanam for preparing Figure 1. Funding from the Faculty Funded Research (FFF), the Swedish Research Council (grants 2016-03398 and 2016-03602), FORMAS (grant 2017-01173), and the Olle Engkvist foundation (grant 18-2006) is recognized. Part of the computations was performed on resources provided by Swedish National Infrastructure for Computing (SNIC) through National Supercomputer Center (NSC) at Linköping University under Project SNIC 2020/13-33, SNIC 2020/5-395, SNIC 2020/5-435, and SNIC 2014/5-33, High Performance Computing Center North (HPC2N) at UmeÅ University under SNIC 2017/3-10, SNIC 2019/5-104, and SNIC 2019/5-116, and Uppsala Multidisciplinary Center for Advanced Computational Science (UPPMAX) at Uppsala University under Project SNIC 2020/15-10 and SNIC 2018/8-321.

REFERENCES

(1) Desiraju, G. R.; Ho, P. S.; Kloo, L.; Legon, A. C.; Marquardt, R.; Metrangolo, P.; Politzer, P.; Resnati, G.; Rissanen, K. Definition of the Halogen Bond (IUPAC Recommendations 2013). *Pure Appl. Chem.* **2013**, *85*, 1711−1713.

(2) Cavallo, G.; Metrangolo, P.; Milani, R.; Pilati, T.; Priimagi, A.; Resnati, G.; Terraneo, G. The Halogen Bond. *Chem. Rev.* **2016**, *116*, 2478−2601.

(3) Turunen, L.; Erdélyi, M. Halogen Bonds of Halonium Ions. *Chem. Soc. Rev.* **2020**, *49*, 2688−2700.

(4) Reiersølmoen, A.; Battaglia, S.; Øien-Ødegaard, S.; Gupta, A.; Fiksdahl, A.; Lindh, R.; Erdélyi, M. Symmetry of Three-Center, Four-Electron Bonds. *Chem. Sci.* **2020**, *11*, 7979−7990.

(5) Carlsson, A.-C. C.; Gräfenstein, J.; Laurila, J. L.; Bergquist, J.; Erdélyi, M. Symmetry of $[N\text{-}X\text{-}N]^+$ Halogen Bonds in Solution. *Chem. Commun.* **2012**, *48*, 1458−1460.

(6) Carlsson, A.-C. C.; Gräfenstein, J.; Budnjo, A.; Laurila, J. L.; Bergquist, J.; Karim, A.; Kleinmaier, R.; Brath, U.; Erdélyi, M. Symmetric Halogen Bonding is Preferred in Solution. *J. Am. Chem. Soc.* **2012**, *134*, 5706−5715.

(7) Carlsson, A.-C. C.; Uhrbom, M.; Karim, A.; Brath, U.; Gräfenstein, J.; Erdélyi, M.; Brath, U.; Erdelyi, M. Solvent Effects on Halogen Bond Symmetry. *CrystEngComm* **2013**, *15*, 3087−3092.

(8) Karim, A.; Reitti, M.; Carlsson, A.-C. C.; Gräfenstein, J.; Erdélyi, M. The Nature of $[N\text{-}Cl\text{-}N]^+$ and $[N\text{-}F\text{-}N]^+$ Halogen Bonds in Solution. *Chem. Sci.* **2014**, *5*, 3226−3233.

(9) Bedin, M.; Karim, A.; Reitti, M.; Carlsson, A.-C. C.; Topić, F.; Cetina, M.; Pan, F.; Havel, V.; Al-Ameri, F.; Sindelar, V.; Rissanen, K.; Gräfenstein, J.; Erdélyi, M. Counterion Influence on the N-I-N Halogen Bond. *Chem. Sci.* **2015**, *6*, 3746−3756.

(10) Carlsson, A.-C. C.; Mehmeti, K.; Uhrbom, M.; Karim, A.; Bedin, M.; Puttreddy, R.; Kleinmaier, R.; Neverov, A. A.; Nekoueishahraki, B.; Gräfenstein, J.; Rissanen, K.; Erdélyi, M. Substituent Effects on the $[N\text{-}I\text{-}N]^+$ Halogen Bond. *J. Am. Chem. Soc.* **2016**, *138*, 9853−9863.

(11) Lindblad, S.; Mehmeti, K.; Veiga, A. X.; Nekoueishahraki, B.; Gräfenstein, J.; Erdélyi, M. Halogen Bond Asymmetry in Solution. *J. Am. Chem. Soc.* **2018**, *140*, 13503−13513.

(12) Ward, J. S.; Fiorini, G.; Frontera, A.; Rissanen, K. Asymmetric $[N\text{-}I\text{-}N]^+$ Halonium Complexes. *Chem. Commun.* **2020**, *56*, 8428−8431.

(13) Aubert, E.; Espinosa, E.; Nicolas, I.; Jeannin, O.; Fourmigué, M. Toward a Reverse Hierarchy of Halogen Bonding between Bromine and Iodine. *Faraday Discuss.* **2017**, *203*, 389−406.

(14) Makhotkina, O.; Lieffrig, J.; Jeannin, O.; Fourmigué, M.; Aubert, E.; Espinosa, E. Cocrystal or Salt: Solid State-Controlled Iodine Shift in Crystalline Halogen-Bonded Systems. *Cryst. Growth Des.* **2015**, *15*, 3464−3473.

(15) Lindblad, S.; Németh, F. B.; Földes, T.; Vanderkooy, A.; Pápai, I.; Erdélyi, M. O-I-O Halogen Bond of Halonium Ions. *Chem. Commun.* **2020**, *56*, 9671−9674.

(16) Koskinen, L.; Jääskeläinen, S.; Hirva, P.; Haukka, M. Tunable Interaction Strength and Nature of the S···Br Halogen Bonds in $[(Thione)Br_2]$ Systems. *Cryst. Growth Des.* **2015**, *15*, 1160−1167.

(17) Koskinen, L.; Hirva, P.; Hasu, A.; Jääskeläinen, S.; Koivistoinen, J.; Pettersson, M.; Haukka, M. Modification of the Supramolecular Structure of [(thione)IY] (Y = Cl, Br) Systems by Cooperation of Strong Halogen Bonds and Hydrogen Bonds. *CrystEngComm* **2015**, *17*, 2718−2727.

(18) Koskinen, L.; Hirva, P.; Kalenius, E.; Jääskeläinen, S.; Rissanen, K.; Haukka, M. Halogen Bonds with Coordinative Nature: Halogen Bonding in a S-I^+-S Iodonium Complex. *CrystEngComm* **2015**, *17*, 1231−1236.

(19) Seppälä, E.; Ruthe, F.; Jeske, J.; du Mont, W.-W.; Jones, P. G. Coordination and Oxidation of Phosphine Selenides with Iodine: From Cation Pairs $[(R_3PSe)_2I^+]_2$ to (iodoseleno)phosphonium Ions $[R_3PSeI]^+$ Existing as Guests in Polyiodide Matrices. *Chem. Commun.* **1999**, 1471−1472.

(20) du Mont, W.-W.; Bätcher, M.; Daniliuc, C.; Devillanova, F. A.; Druckenbrodt, C.; Jeske, J.; Jones, P. G.; Lippolis, V.; Ruthe, F.; Seppälä, E. Soft-Soft Interactions Involving Iodoselenophosphonium Cations: Supramolecular Structures of Iodine Adducts of Bulky Trialkylphosphane Selenides. *Eur. J. Inorg. Chem.* **2008**, 4562−4577.

(21) de Oliveira, G. M.; Faoro, E.; Lang, E. S. New Aryltellurenyl Iodides with Uncommon Valences: Synthetic and Structural Characteristics of $[RTeTeI_2R]$, $[R_2TeTeR_2][Te_4I_{14}]$, and $[RTe(I)I_2]$ (R = 2,6-Dimethoxyphenyl). *Inorg. Chem.* **2009**, *48*, 4607−4609.

(22) Kobra, K.; O'Donnell, S.; Ferrari, A.; McMillen, C. D.; Pennington, W. T. Halogen Bonding and Triiodide Asymmetry in Cocrystals of Triphenylmethylphosphonium Triiodide with Organoiodines. *New J. Chem.* **2018**, *42*, 10518−10528.

(23) Puttreddy, R.; Jurček, O.; Bhowmik, S.; Mäkelä, T.; Rissanen, K. Very strong $-N\text{-}X^+\cdots{}^-O\text{-}N^+$ halogen bonds. *Chem. Commun.* **2016**, *52*, 2338−2341.

(24) Puttreddy, R.; Rautiainen, J. M.; Mäkelä, T.; Rissanen, K. Strong N−X···O −N Halogen Bonds: A Comprehensive Study on N-halosaccharin Pyridine N-oxide Complexes. *Angew. Chem., Int. Ed. Engl.* **2019**, *58*, 18610−18618.

(25) Warzok, U.; Marianski, M.; Hoffmann, W.; Turunen, L.; Rissanen, K.; Pagel, K.; Schalley, C. A. Surprising Solvent-Induced Structural Rearrangements in Large $[N\cdots I^+\cdots N]$ Halogen-Bonded Supramolecular Capsules: An Ion Mobility-Mass Spectrometry Study. *Chem. Sci.* **2018**, *9*, 8343−8351.

(26) Turunen, L.; Peuronen, A.; Forsblom, S.; Kalenius, E.; Lahtinen, M.; Rissanen, K. Tetrameric and Dimeric $[N\cdots I^+\cdots N]$ Halogen-Bonded Supramolecular Cages. *Chem.—Eur. J.* **2017**, *23*, 11714−11718.

(27) Turunen, L.; Warzok, U.; Puttreddy, R.; Beyeh, N. K.; Schalley, C. A.; Rissanen, K. $[N\cdots I^+\cdots N]$ Halogen-Bonded Dimeric Capsules from Tetrakis(3-pyridyl)ethylene Cavitands. *Angew. Chem., Int. Ed. Engl.* **2016**, *55*, 14033−14036.

(28) Vanderkooy, A.; Gupta, A. K.; Földes, T.; Lindblad, S.; Orthaber, A.; Pápai, I.; Erdélyi, M. Halogen Bonding Helicates Encompassing Iodonium Cations. *Angew. Chem., Int. Ed. Engl.* **2019**, *58*, 9012−9016.

(29) Turunen, L.; Warzok, U.; Schalley, C. A.; Rissanen, K. Nanosized $I_{12}L_6$ Molecular Capsules Based on the $[N\cdots I^+\cdots N]$ Halogen Bond. *Chem* **2017**, *3*, 861−869.

(30) Beale, T. M.; Chudzinski, M. G.; Sarwar, M. G.; Taylor, M. S. Halogen Bonding in Solution: Thermodynamics and Applications. *Chem. Soc. Rev.* **2013**, *42*, 1667−1680.

(31) von der Heiden, D.; Vanderkooy, A.; Erdélyi, M. Halogen Bonding in Solution: NMR Spectroscopic Approaches. *Coord. Chem. Rev.* **2020**, *407*, 213147.

(32) Riley, K. E.; Tran, K.-A. Strength, Character, and Directionality of Halogen Bonds involving Cationic Halogen Bond Donors. *Faraday Discuss.* **2017**, *203*, 47−60.

(33) Legon, A. C. Prereactive Complexes of Dihalogens XY with Lewis Bases B in the Gas Phase: A Systematic Case for the Halogen

https://dx.doi.org/10.1021/acs.jctc.0c00860
J. Chem. Theory Comput. 2020, 16, 7690−7701

Analogue B···XY of the Hydrogen Bond B···HX. *Angew. Chem., Int. Ed. Engl.* **1999**, *38*, 2686−2714.
(34) Clark, T.; Hennemann, M.; Murray, J. S.; Politzer, P. Halogen Bonding: the σ-hole. *J. Mol. Model.* **2007**, *13*, 291−296.
(35) Kozuch, S.; Martin, J. M. L. Halogen Bonds: Benchmarks and Theoretical Analysis. *J. Chem. Theory Comput.* **2013**, *9*, 1918−1931.
(36) Engelage, E.; Reinhard, D.; Huber, S. M. Is There a Single Ideal Parameter for Halogen-Bonding-Based Lewis Acidity? *Chem.—Eur. J.* **2020**, *26*, 3843−3861.
(37) Hakkert, S. B.; Erdélyi, M. Halogen Bond Symmetry: the N-X-N Bond. *J. Phys. Org. Chem.* **2015**, *28*, 226−233.
(38) Rissanen, K.; Haukka, M. Halonium Ions as Halogen Bond Donors in the Solid State $[XL_2]Y$ Complexes. *Top. Curr. Chem.* **2015**, *359*, 77−90.
(39) Ebrahimi, A.; Razmazma, H.; Delarami, H. The Nature of Halogen Bonds in $[N\cdots X\cdots N]^+$ Complexes: A Theoretical Study. *Phys. Chem. Res.* **2016**, *4*, 1−15.
(40) Razmazma, H.; Ebrahimi, A. The Effects of Cation-π and Anion-π Interactions on Halogen Bonds in the $[N\cdots X\cdots N]^+$ Complexes: A Comprehensive Theoretical Study. *J. Mol. Graph. Model.* **2018**, *84*, 134−144.
(41) Nguyen, H. T.; Nguyen, D. D.; Spanget-Larsen, J. Ionic Reaction Products of Iodine with Pyridine, 4-methylpyridine, and 4-tert-butylpyridine in a Polyethylene Matrix. A FTIR Polarization Spectroscopic Investigation. *Chem. Phys. Lett.* **2019**, *716*, 119−125.
(42) Georgiou, D. C.; Butler, P.; Browne, E. C.; Wilson, D. J. D.; Dutton, J. L. On the Bonding in Bis-pyridine Iodonium Cations. *Aust. J. Chem.* **2013**, *66*, 1179−1188.
(43) Gräfenstein, J.; Cremer, D. The Self-Interaction Error and the Description of Non-Dynamic Electron Correlation in Density Functional Theory. *Theor. Chem. Acc.* **2009**, *123*, 171−182.
(44) Becke, A. D. A Real-Space Model of Nondynamical Correlation. *J. Chem. Phys.* **2003**, *119*, 2972−2977.
(45) Gräfenstein, J. Efficient Calculation of NMR Isotopic Shifts: Difference-Dedicated Vibrational Perturbation Theory. *J. Chem. Phys.* **2019**, *151*, 244120.
(46) Gräfenstein, J. The Structure of the "Vibration Hole" around an Isotopic Substitution—Implications for the Calculation of Nuclear Magnetic Resonance (NMR) Isotopic Shifts. *Molecules* **2019**, *25*, 2915.
(47) Ghosh, S.; Bhattacharyya, S.; Wategaonkar, S. Dissociation Energies of Sulfur-Centered Hydrogen-Bonded Complexes. *J. Phys. Chem. A* **2015**, *119*, 10863−10870.
(48) Setiawan, D.; Sethio, D.; Cremer, D.; Kraka, E. From Strong to Weak NF Bonds: On the Design of a New Class of Fluorinating Agents. *Phys. Chem. Chem. Phys.* **2018**, *20*, 23913−23927.
(49) Forni, A.; Pieraccini, S.; Franchini, D.; Sironi, M. Assessment of DFT Functionals for QTAIM Topological Analysis of Halogen Bonds with Benzene. *J. Phys. Chem. A* **2016**, *120*, 9071−9080.
(50) Tomasi, J.; Mennucci, B.; Cammi, R. Quantum Mechanical Continuum Solvation Models. *Chem. Rev.* **2005**, *105*, 2999−3094.
(51) Bondi, A. van der Waals Volumes and Radii. *J. Phys. Chem.* **1964**, *68*, 441−451.
(52) Willoughby, P. H.; Jansma, M. J.; Hoye, T. R. A Guide to Small-Molecule Structure Assignment through Computation of (^{1}H and ^{13}C) NMR Chemical Shifts. *Nat. Protoc.* **2014**, *9*, 643−660.
(53) Ditchfield, R. Molecular Orbital Theory of Magnetic Shielding and Magnetic Susceptibility. *J. Chem. Phys.* **1972**, *56*, 5688−5691.
(54) Ditchfield, R. Self-Consistent Perturbation Theory of Diamagnetism. *Mol. Phys.* **1974**, *27*, 789−807.
(55) Wolinski, K.; Hinton, J. F.; Pulay, P. Efficient Implementation of the Gauge-Independent Atomic Orbital Method for NMR Chemical Shift Calculations. *J. Am. Chem. Soc.* **1990**, *112*, 8251−8260.
(56) Roothaan, C. C. J. New Developments in Molecular Orbital Theory. *Rev. Mod. Phys.* **1951**, *23*, 69−89.
(57) Møller, C.; Plesset, M. S. Note on An Approximation Treatment for Many-Electron Systems. *Phys. Rev.* **1934**, *46*, 618−622.
(58) Kohn, W.; Sham, L. J. Self-Consistent Equations Including Exchange and Correlation Effects. *Phys. Rev.* **1965**, *140*, A1133−A1138.
(59) Vosko, S. H.; Wilk, L.; Nusair, M. Accurate Spin-Dependent Electron Liquid Correlation Energies for Local Spin Density Calculations: A Critical Analysis. *Can. J. Phys.* **1980**, *58*, 1200−1211.
(60) Perdew, J. P.; Burke, K.; Ernzerhof, M. Generalized Gradient Approximation Made Simple. *Phys. Rev. Lett.* **1996**, *77*, 3865−3868.
(61) Perdew, J. P.; Burke, K.; Ernzerhof, M. Generalized Gradient Approximation Made Simple [Phys. Rev. Lett. 77, 3865 (1996)]. *Phys. Rev. Lett.* **1997**, *78*, 1396.
(62) Tao, J.; Perdew, J. P.; Staroverov, V. N.; Scuseria, G. E. Climbing the Density Functional Ladder: Nonempirical Meta-Generalized Gradient Approximation Designed for Molecules and Solids. *Phys. Rev. Lett.* **2003**, *91*, 146401.
(63) Becke, A. D. Density-Functional Exchange-Energy Approximation with Correct Asymptotic Behavior. *Phys. Rev. A: At., Mol., Opt. Phys.* **1988**, *38*, 3098−3100.
(64) Lee, C.; Yang, W.; Parr, R. G. Development of the Colle-Salvetti Correlation-Energy Formula into a Functional of the Electron Density. *Phys. Rev. B: Condens. Matter Mater. Phys.* **1988**, *37*, 785−789.
(65) Yanai, T.; Tew, D. P.; Handy, N. C. A New Hybrid Exchange-Correlation Functional Using the Coulomb-Attenuating Method (CAM-B3LYP). *Chem. Phys. Lett.* **2004**, *393*, 51−57.
(66) Vydrov, O. A.; Scuseria, G. E. Assessment of a Long-Range Corrected Hybrid Functional. *J. Chem. Phys.* **2006**, *125*, 234109.
(67) Vydrov, O. A.; Heyd, J.; Krukau, A. V.; Scuseria, G. E. Importance of Short-Range Versus Long-Range Hartree-Fock Exchange for the Performance of Hybrid Density Functionals. *J. Chem. Phys.* **2006**, *125*, 074106.
(68) Vydrov, O. A.; Scuseria, G. E.; Perdew, J. P. Tests of Functionals for Systems with Fractional Electron Number. *J. Chem. Phys.* **2007**, *126*, 154109.
(69) Chai, J.-D.; Head-Gordon, M. Long-Range Corrected Hybrid Density Functionals with Damped Atom-Atom Dispersion Corrections. *Phys. Chem. Chem. Phys.* **2008**, *10*, 6615.
(70) Iikura, H.; Tsuneda, T.; Yanai, T.; Hirao, K. A Long-Range Correction Scheme for Generalized-Gradient-Approximation Exchange Functionals. *J. Chem. Phys.* **2001**, *115*, 3540−3544.
(71) Zhao, Y.; Truhlar, D. G. A New Local Density Functional for Main-Group Thermochemistry, Transition Metal Bonding, Thermochemical Kinetics, and Noncovalent Interactions. *J. Chem. Phys.* **2006**, *125*, 194101.
(72) Zhao, Y.; Truhlar, D. G. The M06 Suite of Density Functionals for Main Group Thermochemistry, Thermochemical Kinetics, Noncovalent Interactions, Excited States, and Transition Elements: Two New Functionals and Systematic Testing of Four M06-class Functionals and 12 Other Functionals. *Theor. Chem. Acc.* **2007**, *120*, 215−241.
(73) Zhao, Y.; Truhlar, D. G. Density Functional for Spectroscopy: No Long-Range Self-Interaction Error, Good Performance for Rydberg and Charge-Transfer States, and Better Performance on Average than B3LYP for Ground States. *J. Phys. Chem. A* **2006**, *110*, 13126−13130.
(74) McLean, A. D.; Chandler, G. S. Contracted Gaussian Basis Sets for Molecular Calculations. I. Second Row Atoms, Z=11-18. *J. Chem. Phys.* **1980**, *72*, 5639−5648.
(75) Krishnan, R.; Binkley, J. S.; Seeger, R.; Pople, J. A. Self-consistent Molecular Orbital Methods. XX. A Basis Set for Correlated Wave Functions. *J. Chem. Phys.* **1980**, *72*, 650−654.
(76) Weigend, F.; Ahlrichs, R. Balanced Basis Sets of Split Valence, Triple Zeta Valence and Quadruple Zeta Valence Quality for H to Rn: Design and Assessment of Accuracy. *Phys. Chem. Chem. Phys.* **2005**, *7*, 3297.
(77) Weigend, F. Accurate Coulomb-Fitting Basis Sets for H to Rn. *Phys. Chem. Chem. Phys.* **2006**, *8*, 1057.

https://dx.doi.org/10.1021/acs.jctc.0c00860
J. Chem. Theory Comput. 2020, 16, 7690−7701

(78) Dunning, T. H. Gaussian Basis Sets for Use in Correlated Molecular Calculations. I. The Atoms Boron through Neon and Hydrogen. *J. Chem. Phys.* **1989**, *90*, 1007−1023.
(79) Woon, D. E.; Dunning, T. H. Gaussian Basis Sets for Use in Correlated Molecular Calculations. V. Core-valence basis sets for boron through neon. *J. Chem. Phys.* **1995**, *103*, 4572−4585.
(80) Peterson, K. A. Systematically Convergent Basis Sets with Relativistic Pseudopotentials. I. Correlation Consistent Basis Sets for the post-d Group 13-15 Elements. *J. Chem. Phys.* **2003**, *119*, 11099−11112.
(81) Peterson, K. A.; Figgen, D.; Goll, E.; Stoll, H.; Dolg, M. Systematically Convergent Basis Sets with Relativistic Pseudopotentials. II. Small-core Pseudopotentials and Correlation Consistent Basis Sets for the post-d Group 16-18 Elements. *J. Chem. Phys.* **2003**, *119*, 11113−11123.
(82) Hay, P. J.; Wadt, W. R. Ab Initio Effective Core Potentials for Molecular Calculations. Potentials for the Transition Metal Atoms Sc to Hg. *J. Chem. Phys.* **1985**, *82*, 270−283.
(83) Pazderski, L. ^{15}N NMR Coordination Shifts in Pd(II), Pt(II), Au(III), Co(III), Rh(III), Ir(III), Pd(IV), and Pt(IV) Complexes with pyridine, 2,2′-bipyridine, 1,10-phenanthroline, quinoline, isoquinoline, 2,2′-biquinoline, 2,2′:6′, 2′-terpyridine and their alkyl or aryl. *Magn. Reson. Chem.* **2008**, *46*, S3−S15.
(84) Frisch, M. J.; Trucks, G. W.; Schlegel, H. B.; Scuseria, G. E.; Robb, M. A.; Cheeseman, J. R.; Scalmani, G.; Barone, V.; Petersson, G. A.; Nakatsuji, H.; Li, X.; Caricato, M.; Marenich, A. V.; Bloino, J.; Janesko, B. G.; Gomperts, R.; Mennucci, B.; Hratchian, H. P.; Ortiz, J. V.; Izmaylov, A. F.; Sonnenberg, J. L.; Williams-Young, D.; Ding, F.; Lipparini, F.; Egidi, F.; Goings, J.; Peng, B.; Petrone, A.; Henderson, T.; Ranasinghe, D.; Zakrzewski, V. G.; Gao, J.; Rega, N.; Zheng, G.; Liang, W.; Hada, M.; Ehara, M.; Toyota, K.; Fukuda, R.; Hasegawa, J.; Ishida, M.; Nakajima, T.; Honda, Y.; Kitao, O.; Nakai, H.; Vreven, T.; Throssell, K.; Montgomery, J. A., Jr; Peralta, J. E.; Ogliaro, F.; Bearpark, M. J.; Heyd, J. J.; Brothers, E. N.; Kudin, K. N.; Staroverov, V. N.; Keith, T. A.; Kobayashi, R.; Normand, J.; Raghavachari, K.; Rendell, A. P.; Burant, J. C.; Iyengar, S. S.; Tomasi, J.; Cossi, M.; Millam, J. M.; Klene, M.; Adamo, C.; Cammi, R.; Ochterski, J. W.; Martin, R. L.; Morokuma, K.; Farkas, O.; Foresman, J. B.; Fox, D. J. *Gaussian 16* Revision C.01.; Gaussian Inc.: Wallingford CT, 2016.
(85) Gräfenstein, J.; Cremer, D. Efficient Density-Functional Theory Integrations by Locally Augmented Radial Grids. *J. Chem. Phys.* **2007**, *127*, 164113.
(86) Glendening, E. D.; Badenhoop, J. K.; Reed, A. E.; Carpenter, J. E.; Bohmann, J. A.; Morales, C. M.; Karafiloglou, P.; Landis, C. R.; Weinhold, F. *NBO7*; Theoretical Chemistry Institute, University of Wisconsin: Madison, 2018.
(87) Glendening, E. D.; Landis, C. R.; Weinhold, F. NBO 6.0: Natural Bond Orbital Analysis Program. *J. Comput. Chem.* **2013**, *34*, 1429−1437.
(88) Stoychev, G. L.; Auer, A. A.; Izsák, R.; Neese, F. Self-Consistent Field Calculation of Nuclear Magnetic Resonance Chemical Shielding Constants Using Gauge-Including Atomic Orbitals and Approximate Two-Electron Integrals. *J. Chem. Theory Comput.* **2018**, *14*, 619−637.
(89) Reitti, M. The X^+ and X^{3+} Halogen Bonds. M.Sc. Thesis, Department of Chemistry and Molecular Biology, University of Gothenburg, Gothenburg, 2014.
(90) Teale, A. M.; Lutnæs, O. B.; Helgaker, T.; Tozer, D. J.; Gauss, J. Benchmarking Density-Functional Theory Calculations of NMR Shielding Constants and Spin-Rotation Constants using Accurate Coupled-Cluster Calculations. *J. Chem. Phys.* **2013**, *138*, 024111.
(91) Álvarez-Rúa, C.; García-Granda, S.; Ballesteros, A.; González-Bobes, F.; González, J. M. Bis(pyridine)iodonium(I) Tetrafluoroborate. *Acta Crystallogr., Sect. E: Struct. Rep. Online* **2002**, *58*, o1381−o1383.
(92) Flaig, D.; Maurer, M.; Hanni, M.; Braunger, K.; Kick, L.; Thubauville, M.; Ochsenfeld, C. Benchmarking Hydrogen and Carbon NMR Chemical Shifts at HF, DFT, and MP2 Levels. *J. Chem. Theory Comput.* **2014**, *10*, 572−578.
(93) Reimann, S.; Ekström, U.; Stopkowicz, S.; Teale, A. M.; Borgoo, A.; Helgaker, T. The Importance of Current Contributions to Shielding Constants in Density-Functional Theory. *Phys. Chem. Chem. Phys.* **2015**, *17*, 18834−18842.
(94) Yesiltepe, Y.; Nuñez, J. R.; Colby, S. M.; Thomas, D. G.; Borkum, M. I.; Reardon, P. N.; Washton, N. M.; Metz, T. O.; Teeguarden, J. G.; Govind, N.; Renslow, R. S. An Automated Framework for NMR Chemical Shift Calculations of Small Organic Molecules. *J. Cheminf.* **2018**, *10*, 52.
(95) Alipour, M. In Search of the Appropriate Theoretically Justified Mixing Coefficient in Parameter-free Hybrid Functionals for Computing the NMR Parameters. *RSC Adv.* **2015**, *5*, 4737−4746.
(96) Wu, A.; Zhang, Y.; Xu, X.; Yan, Y. Systematic Studies on the Computation of Nuclear Magnetic Resonance Shielding Constants and Chemical Shifts: The Density Functional Models. *J. Comput. Chem.* **2007**, *28*, 2431−2442.
(97) Giesen, D. J.; Zumbulyadis, N. A Hybrid Quantum Mechanical and Empirical Model for the Prediction of Isotropic ^{13}C Shielding Constants of Organic Molecules. *Phys. Chem. Chem. Phys.* **2002**, *4*, 5498−5507.
(98) Zhang, D.; Truhlar, D. G. Unmasking Static Correlation Error in Hybrid Kohn-Sham Density Functional Theory. *J. Chem. Theory Comput.* **2020**, *16*, 5432−5440.
(99) Gauss, J. Calculation of NMR Chemical Shifts at Second-Order Many-Body Perturbation Theory using Gauge-Including Atomic Orbitals. *Chem. Phys. Lett.* **1992**, *191*, 614−620.
(100) Gauss, J. Effects of Electron Correlation in the Calculation of Nuclear Magnetic Resonance Chemical Shifts. *J. Chem. Phys.* **1993**, *99*, 3629−3643.
(101) Auer, A. A.; Gauss, J.; Stanton, J. F. Quantitative Prediction of Gas-Phase ^{13}C Nuclear Magnetic Shielding Constants. *J. Chem. Phys.* **2003**, *118*, 10407−10417.
(102) Gregušová, A.; Perera, S. A.; Bartlett, R. J. Accuracy of Computed ^{15}N Nuclear Magnetic Resonance Chemical Shifts. *J. Chem. Theory Comput.* **2010**, *6*, 1228−1239.
(103) Prochnow, E.; Auer, A. A. Quantitative Prediction of Gas-Phase ^{15}N and ^{31}P Nuclear Magnetic Shielding Constants. *J. Chem. Phys.* **2010**, *132*, 064109.
(104) Xin, D.; Sader, C. A.; Fischer, U.; Wagner, K.; Jones, P.-J.; Xing, M.; Fandrick, K. R.; Gonnella, N. C. Systematic Investigation of DFT-GIAO ^{15}N NMR Chemical Shift Prediction using B3LYP/cc-pVDZ: Application to Studies of Regioisomers, Tautomers, Protonation States and N-oxides. *Org. Biomol. Chem.* **2017**, *15*, 928−936.
(105) Samultsev, D. O.; Semenov, V. A.; Krivdin, L. B. On the Accuracy of the GIAO-DFT Calculation of ^{15}N NMR Chemical Shifts of the Nitrogen-containing Heterocycles - A Gateway to Better Agreement with Experiment at Lower Computational Cost. *Magn. Reson. Chem.* **2014**, *52*, 222−230.
(106) Isborn, C. M.; Mar, B. D.; Curchod, B. F. E.; Tavernelli, I.; Martínez, T. J. The Charge Transfer Problem in Density Functional Theory Calculations of Aqueously Solvated Molecules. *J. Phys. Chem. B* **2013**, *117*, 12189−12201.
(107) Setiawan, D.; Sethio, D.; Martoprawiro, M. A.; Filatov, M. Formation of Bonded Exciplex in the Excited States of Dicyanoanthracene-Pyridine System: Time Dependent Density Functional Theory Study. *Proceedings of the 2011 2nd International Congress on Computer Applications and Computational Science. Advances in Intelligent and Soft Computing*; Springer, 2012; vol. *145*, pp 403−409, DOI: 10.1007/978-3-642-28308-6_55.
(108) Mulliken, R. S. Charge-Transfer Band of the Pyridine-Iodine Complex. *J. Am. Chem. Soc.* **1969**, *91*, 1237.
(109) Mardirossian, N.; Head-Gordon, M. How Accurate Are the Minnesota Density Functionals for Noncovalent Interactions, Isomerization Energies, Thermochemistry, and Barrier Heights Involving Molecules Composed of Main-Group Elements? *J. Chem. Theory Comput.* **2016**, *12*, 4303−4325.
(110) Iron, M. A. Evaluation of the Factors Impacting the Accuracy of ^{13}C NMR Chemical Shift Predictions using Density Functional

https://dx.doi.org/10.1021/acs.jctc.0c00860
J. Chem. Theory Comput. 2020, 16, 7690−7701

Theory-The Advantage of Long-Range Corrected Functionals. *J. Chem. Theory Comput.* **2017**, *13*, 5798−5819.
(111) Toomsalu, E.; Burk, P. Critical Test of Some Computational Methods for Prediction of NMR ^{1}H and ^{13}C Chemical Shifts. *J. Mol. Model.* **2015**, *21*, 244.
(112) Jensen, F. Basis Set Convergence of Nuclear Magnetic Shielding Constants Calculated by Density Functional Methods. *J. Chem. Theory Comput.* **2008**, *4*, 719−727.
(113) Jensen, F. Segmented Contracted Basis Sets Optimized for Nuclear Magnetic Shielding. *J. Chem. Theory Comput.* **2015**, *11*, 132−138.
(114) Perdew, J. P.; Schmidt, K. Jacob's Ladder of Density Functional Approximations for the Exchange-Correlation Energy. *AIP Conf. Proc.* **2001**, *577*, 1−20.
(115) Stoychev, G. L.; Auer, A. A.; Neese, F. Efficient and Accurate Prediction of Nuclear Magnetic Resonance Shielding Tensors with Double-Hybrid Density Functional Theory. *J. Chem. Theory Comput.* **2018**, *14*, 4756−4771.

https://dx.doi.org/10.1021/acs.jctc.0c00860
J. Chem. Theory Comput. 2020, 16, 7690−7701